Native like structure and stability of apo AI in a *n*-propanol/water solution as determined by ^{13}C NMR

Arnaud Leroy[a,*], Guy Lippens[b], Jean-Michel Wieruszeski[b], Henri-Joseph Parra[a], Jean-Charles Fruchart[a]

[a]*SERLIA et INSERM U 325 Institut Pasteur de Lille, 1 rue du professeur Calmette, 59019 Lille CEDEX, France*
[b]*URA 1309 CNRS–SCBM, Institut Pasteur de Lille, 1 rue du Professeur Calmette, 59019 Lille CEDEX, France*

Received 23 January 1995

Abstract To elucidate the molecular details of the conformation of apolipoprotein AI (apo AI), we have developed an approach related to the solubilization of this protein in 30% *n*-propanol. We have previously reported the promotion of a native-like structure for apo AI solubilized in *n*-propanol, as depicted by circular dichroism, fluorescence, and limited proteolytic digestion as compared to the lipid associated form of apo AI. In the present study, we labeled the Lys residues of apo AI with ^{13}C by reductive methylation and used ^{13}C NMR to confirm the formation of a native-like structure of apo AI in this environment. Furthermore, by the above criteria (circular dichroism and ^{13}C NMR) and by using urea and temperature as denaturing agents, we show that the denaturation of the native-like structure of apo AI in *n*-propanol is a biphasic process. These studies show that in 30% *n*-propanol, apo AI contains two independently folded structural domains, of markedly different stabilities that might correspond to the amino-terminal and the carboxy-terminal halves of the molecule.

Key words: Apolipoprotein AI (Human); *n*-Propanol; Conformation; ^{13}C dimethyl-Lys NMR

1. Introduction

The function of plasma lipoproteins is to transport lipids in the blood. They are macromolecular complexes containing a variety of lipids and proteins. The protein components of the lipoprotein complex are referred to as apolipoproteins (apo) and bind to the monolayer of phospholipid located on the surface of the various classes of lipoprotein particles. Apolipoproteins regulate lipoprotein metabolism and control the transport and redistribution of lipids among tissues and cells [1]. With the exception of apo B, all the apolipoproteins are water soluble in the absence of detergents or denaturants. The water soluble forms tend to exhibit a high degree of α-helical content, particularly when associated with lipid [2].

Apolipoprotein AI is the primary constituent of high density lipoproteins (HDL). Previous observations suggest that the structure of this protein may be critical to a number of regulatory mechanisms that affect the metabolism of HDL and cholesterol homeotasis. The molecular details of how a change in apo AI affects the microstructure of HDL have been difficult to resolve. Detailed information about apo AI conformation will be needed to elucidate clearly the structure–function relationships that may be central to HDL metabolism.

Except for the N-terminal thrombolytic fragment of apo E [3,4] and the human apo CI [5], that have been crystallized, there is not a lot of information available to-day about the tertiary structure of human apolipoprotein. This can probably be attributed to difficulties in crystallization due to the flexible nature of the protein.

As previously reported by us [6], by varying the concentration of *n*-propanol between 0 to 90% and by measuring the ellipticity of apo AI at 222 nm, we observed a maximal α-helical content close to 80% for apo AI in a 30% *n*-propanol solution compared to approximately 50% for apo AI in aqueous solution. We also observed a maximal ellipticity of apo AI at 290.6 nm in 30% *n*-propanol by circular dichroism in the near UV. For a lipid asssociated form of apo AI (discoidal POPC reconstituted HDL 96 Å) and apo AI solubilized in 30% *n*-propanol we obtained similar slow kinetics and products of proteolysis, whereas a different proteolysis behaviour was observed for apo AI in aqueous solution. Cross-linking experiments revealed that dimers of apo AI exist in *n*-propanol and in reconstituted HDL 96 Å, in contrast to dimers plus multimeric aggregates in aqueous buffer. From these results we concluded that in 30% *n*-propanol the structure of apo AI approaches that of 'native' lipid bound apo AI [7], in contrast to its structure in the aqueous solution [6].

Sparks et al. [8] reported that apo AI, maximally ^{13}C labeled by reductive methylation of its primary amine groups (α-NH-asp terminus and ε-Lys residues), was able to associate normally with lipids compared to unlabeled apo AI. They observed no difference in the rate and the extent of reassociation with the lipids nor in the composition or the size of the complexes formed. Furthermore, Jonas et al. [9] have shown that 84% methylation of apo AI residues has no effect on the activation of lecithin:cholesterol acyltransferase. Therefore, the reductive methylation of apo AI seems to have no effect on the physicochemical and biological properties of apo AI.

Sparks et al. [8] utilized ^{13}C NMR spectroscopy to probe the structure of apo AI labeled on discoidal and spherical reconstituted HDL of different sizes. By ^{13}C NMR and circular dichroism, these authors observed that the arrangement of apo AI molecules on the lipoprotein surface is a function of the particle size for discs but not for spheres. Their results also suggest that much of apo AI structure on the small spherical

*Corresponding author. Fax: (33) 20 87 73 60.

Abbreviatons: apo AI, apolipoprotein AI; HDL, high density lipoprotein(s); rHDL, reconstituted HDL; POPC, palmitoyl-oleoyl-phosphatidyl-choline; TMSP, trimethyl-silyl-2,2′-3,3′-D-propionic acid, sodium salt; NMR, nuclear magnetic resonance.

SSDI 0014-5793(95)00134-4

HDL is similar to that on the small discoidal HDL for which an identical α-helical content (62%) for apo AI is observed.

The aim of the present study is to determine whether the native-like structure of apo AI in *n*-propanol is closer to the arrangement of apo AI on discoidal or spherical HDL, as assessed by the technique of ^{13}C NMR and the previous results of Sparks et al. [8].

2. Materials and methods

All materials used were reagent grade and were used without further purification. Apo AI concentration was determined by absorption at 280 nm (ε_{280} = 31,720 $M^{-1} \cdot cm^{-1}$ [10]). $H^{13}CHO$ was obtained from Isotec Inc. USA. Deuterium oxide (99.8%) was obtained from the C.E.A. (France). Apo AI was isolated from HDL_3 as described before [11]. HDL_3 (d = 1.12–1.21 g/ml) were isolated from plasma of normolipemic human donors by sequential flotation ultracentrifugation.

2.1. Reductive methylation of apo AI

The labeling of the Lys residues of apo AI With $^{13}CH_3$ groups was accomplished by the reductive methylation procedure of Jentoft and Dearborn [12]. To label all apo AI Lys residues, 11.0 mmol of $NaCNBH_3$/mg of protein was added to apo AI dissolved in cold saline, pH 7.4. The protein concentration was then adjusted to 2.75 mg/ml with excess cold saline, 8.9 μmol of $H^{13}CHO$/mg of apo AI was added and the mixture was incubated for 18 h et 4°C. The reaction was terminated by dialysis against saline at 4°C.

2.2. Circular dichroism measurements

To assess secondary structure, circular dichroism spectra of apo AI were recorded on a Model CD6 Jobin Yvon, ISA spectropolarimeter (Longjumeau, France) calibrated with a 0.1% (w/v) d-10-camphorsulfonic acid solution. CD spectra were measured from 200 to 250 nm in a 1 mm path length quartz cuvette with sample protein concentrations of 0.2 mg/ml. Thermal denaturation of apo AI was monitored by the change with temperature of the molar ellipticity at 222 nm. Sample temperature was maintained at 4°C to 90°C ± 0.5°C in a jacketed 0.1 cm path length quartz cuvette by a Haake F4 circulation pump (Haake, Saddle Brook, NJ) and temperature was monitored inside the cuvette with a thermocouple. Contents of α-helical structure in apo AI were estimated from the molar ellipticities at 222 nm ($[\Theta]_{222}$) using the empirical expression of Chen et al. [13]:

$$[\Theta]_{222} = -30300 f_H - 2340$$

f_H is the fraction of α-helical structure.

2.3. NMR measurements

We prepared 0.5 ml samples of apo AI at concentrations of 2 mg/ml in a): 0.5 ml of 0.02 M sodium borate, 0.15 M sodium chloride, 1 mM EDTA, and 0.02% NaN_3, pH 8.5; or in b): the same components in 30% *n*-propanol/H_2O (V/V). We added 50 μl of D_2O (as the NMR lock compound) and 10 μl of 50 mM TMSP (as the internal reference) to obtain a final volume of 560 μl. ^{13}C NMR spectra were recorded on a Brucker DMX spectrometer at 150 MHz (Bruker-France, Wissembourg), using a WALTZ sequence for proton decoupling. Sweep widths of 250 ppm were observed by using a 30° pulse of 5.5 μs duration and a recycling time of 1.6 s. Free induction decays were accumulated over 24000 scans with 32768 complex points and Fourier transformed after weighting with a 1 Hz line broadening filter. For the samples containing 30% *n*-propanol, we had severe difficulties with the shimming of the magnet due to the increased viscosity of the solvent. Therefore, we shimmed on a D_2O sample with exactly the same volume as the sample considered. A second problem was the signal of the *n*-propanol natural abundance ^{13}C nuclei, necessitating a slight decrease of the receiver gain. Sample temperatures were controlled with the Bruker thermostat at ±0.5°C.

The pH (uncorrected for D_2O) was measured using an ORION RESEARCH pH meter (Cambridge, Mass); pH titration experiments were performed on the same samples by adding small quantities of 1 M HCl or NaOH solution.

3. Results and discussion

3.1. Reductive methylation of apo AI

To label all the Lys residues of apo AI with $^{13}CH_3$ groups we followed the procedure of Jentoft and Dearborn [12] that was adapted and optimized for apo AI in order to yield routinely a dimethylation of 95 to 100% of the Lys residues [8]. The upfield regions of the ^{13}C NMR spectrum obtained at pH 7.7 for free apo AI at 4°C is shown in Fig. 1 and displays three peaks. This spectrum is quite similar to the spectrum reported and obtained at 37°C by Sparks et al. [8] except for the global downfield shift (2.7 ppm) of the peaks that might be related to the choice of TMSP as an internal reference for this study and 1,4-dioxane as an external reference in the study of Sparks et al. [8]. The well resolved predominant resonance (peak a, Fig. 1) at 45.4 ppm represents the [^{13}C]dimethyl-Lys residues of apo AI as previously reported [8]. The two smaller resonances observed in the spectrum for apo AI in Fig. 1 correspond to the [^{13}C]dimethyl-Asp NH_2-terminal (43.9 ppm, peak b) and to [^{13}C] monomethyl-Lys (35.6 ppm, peak c) as assigned by Jentoft et al. [14]. The intensity of the monomethyl-Lys resonance is less than 3% that of the dimethyl Lys resonance, indicating that the majority of the Lys residues are dimethylated during the reductive methylation procedure.

3.2. Apo AI Lys microenvironment in aqueous versus 30% n-propanol solution at different pH

As the pH is raised from 7.7 to 8.5 and to 10 (Fig. 2), the ^{13}C dimethyl-Lys resonance at 4°C for both aqueous and *n*-propanol solutions of apo AI becomes an increasingly complex envelope. At pH 10, substantial differences are apparent in the chemical shifts and in the amplitudes of the individual Lys resonance peaks that constitute the complex envelope of the dimethyl-Lys resonance, from 45 to 46.5 ppm for apo AI in aqueous solution and from 45 to 47 ppm for apo AI in *n*-propanol solution (Fig. 2). Since these changes are reversible and since the increase in pH from 7.7 to 10 has no significant effect on the protein secondary structure (as depicted by circular dichroism spectroscopy), this indicates that the dimethyl-Lys residues in apo AI exist in different microenvironments, each of which has a different ionization behavior [8]. At pH 7.7 and 4°C the dimethyl-Lys envelope contains a predominant peak at chemical shift (δ) 45.36 ppm and 45.28 ppm for apo AI

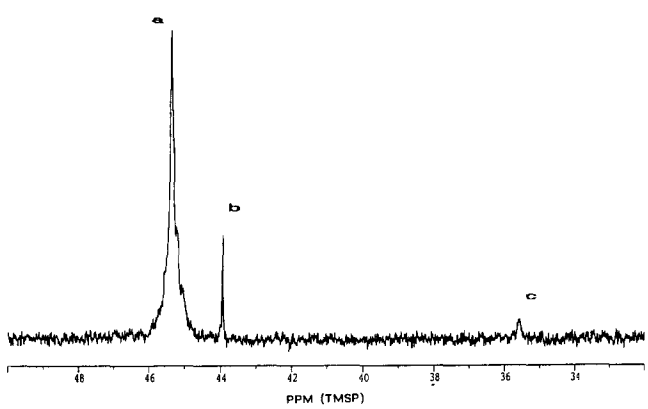

Fig. 1. ^{13}C NMR spectra at 150 MHz of ^{13}C dimethylated apo AI at pH 7.7. The upfield region of the proton decoupled ^{13}C NMR spectra obtained at 4°c for apo AI (2 mg/ml, 24000 acquisitions) are shown.

in aqueous and *n*-propanol solution, respectively. At pH 10 and 4°C the dimethyl-Lys envelope contains a predominant peak at δ 45.51 ppm and 46 ppm for apo AI in aqueous and *n*-propanol solution, respectively. Notable among these spectra are the behavior of the dimethyl N-terminal-Asp residue of apo AI when the pH increases. The chemical shifts for the NH_2-terminal α-amino group of apo AI, solubilized in aqueous or in *n*-propanol solution, move in an upfield direction with increases in pH in contrast to the dimethyl-Lys ε-amino groups resonances which all shift downfield as the pH is raised. Similar behavior has been observed by Sparks et al. [8] with apo AI in aqueous solution or associated with lipid.

Studies have shown that the nuclear overhauser enhancement factors are constant for dimethyl-Lys resonances in different proteins regardless of their titration characteristics [15,16]. It follows that the relative integrals of the deconvoluted dimethyl-Lys resonances will closely represent the relative number of Lys residues contributing to the individual signals. In this study we did not try to deconvolute the dimethyl-Lys resonances recorded at pH 10 using a Lorentzian algorithm as was done by Sparks et al. [8]. In our future studies we will repeat the same experiment but using a wide bore broad band inverse (BBI) Bruker probe accepting a sample tube with diameter of 8 mm instead of 5 mm in order to increase the signal/noise ratio,

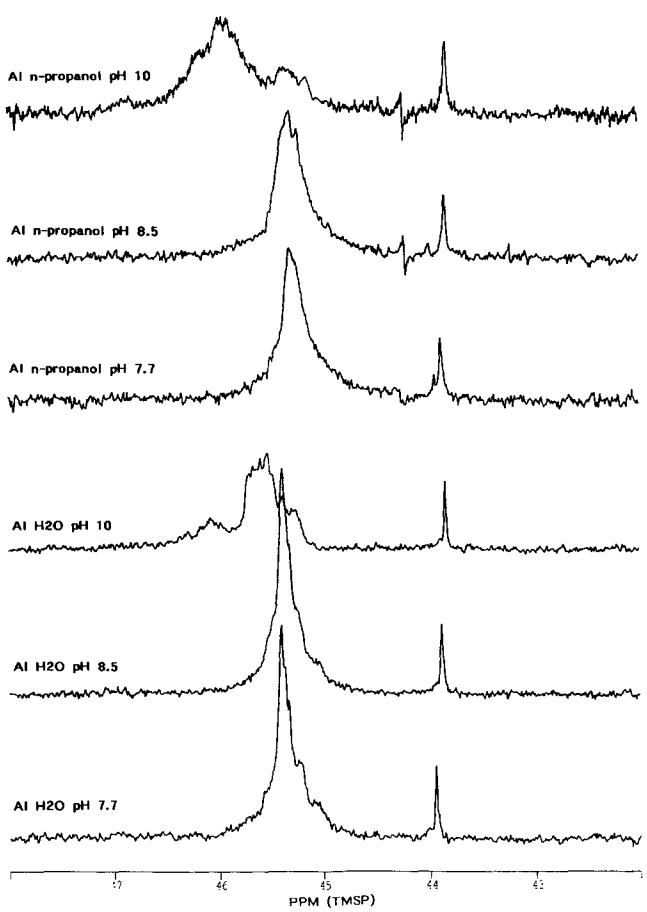

Fig. 2. Effect of pH on the ^{13}C NMR spectra of ^{13}C dimethylated apo AI solubilized in 0.02 M sodium borate, 0.15 M sodium chloride, 1 mM EDTA, and 0.02% NaN_3 (3 spectra at the bottom of the figure); or apo AI in the same components in 30% *n*-propanol/H_2O (3 spectra at the top of the figure). The temperature was maintained at 4°C during the acquisition of these spectra.

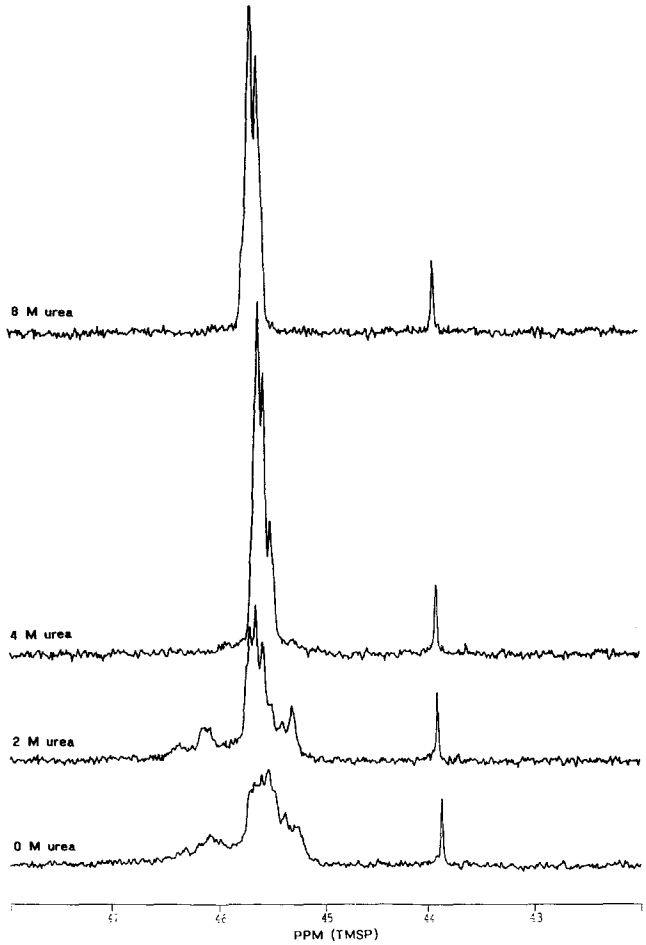

Fig. 3. Effect of urea concentration (0, 2, 4 and 8 M) on the ^{13}C NMR spectra of ^{13}C dimethylated apo AI solubilized in 0.02 M sodium borate, 0.15 M sodium chloride, 1 mM EDTA, and 0.02% NaN_3. The temperature was maintained at 4°C and the pH at 10 during the acquisition of these spectra.

thus permitting accurate deconvolution and fitting of the complex spectrum of the dimethyl-Lys residues to a multiple Lorenzantian population of resonances.

Nevertheless, we obtain a relative intensity of 20 for the ratio of the integrated areas for the dimethyl-Lys resonances and the dimethyl-terminal amino group resonance of apo AI, from the spectra recorded at different pH and in different environments under our conditions (Fig. 2). This ratio is consistent with apo AI being more than 90% labeled and reflects the 21/1 ratio of dimethyl-Lys to NH_2-terminal dimethyl amino groups.

3.3. *Effect of urea concentration on Apo AI Lys microenvironment*

At 4°C, pH 10 and in the absence of urea, the ^{13}C dimethyl-Lys resonance of apo AI solubilized in aqueous solution is a complex envelope that consists in a broad resonance from 45 ppm to 46.53 ppm (see spectrum at the bottom of Fig. 3). This multiple-peak spectrum is a result of the different microenvironments of the dimethyl-Lys residues.

Under similar conditions, but in the presence of 8 M urea, ^{13}C-labeled apo AI solubilized in aqueous solution gives a sharp

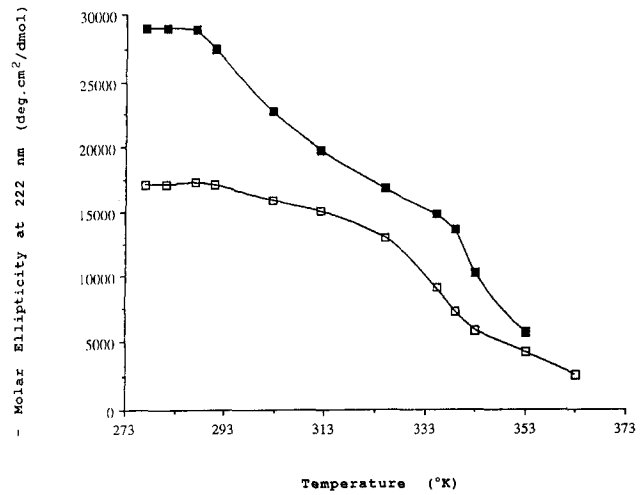

Fig. 4. Effect of temperature on the molar ellipticity at 222 nm of apo AI. Aliquots of apo AI in aqueous (□) and in 30% *n*-propanol (■) solution were maintained by a Haake F4 water bath at various T° from 277 to 363 ± 0.5°K in a jacketed 0.1 cm path length quartz cuvette. CD spectra were measured at 5–10°C intervals with sample protein concentration of 0.2 mg/ml.

resonance envelope with a predominant peak at 45.71 ppm with a secondary peak at 45.63 ppm (spectrum at the top of Fig. 3). This occurs because apo AI loses its secondary and tertiary structural organisation in 8 M urea and therefore, causes the multiple peaks of dimethyl-Lys to collapse into a single peak. A similar behavior is observed in the presence of 30% *n*-propanol and 8 M urea (data not shown).

3.4. Effect of the temperature on the circular dichroism of apo AI solubilized in aqueous versus 30% n-propanol solution

To examine the stability of human apo AI in solution, the effect of temperature (from 281°K to 363°K) on the secondary structure of the protein was investigated. Fig. 4 illustrates the relationship between the temperature and the mean residue ellipticity at 222 nm for apo AI solubilized in aqueous and in *n*-propanol solution. The initial results, $[\Theta]_{222} = -29000$ degrees · cm^2 · dmol^{-1} and $[\Theta_{222} = -17000$ degrees · cm^2 · dmol^{-1}, for apo AI in 30% *n*-propanol solution and apo AI in aqueous solution, respectively, indicated that apo AI in *n*-propanol had more degree of secondary structure than apo AI solubilized in water. Using the expression of Chen et al. [13] we can estimate from Fig. 4 the α-helical content at 281°K of apo AI solubilized in aqueous and in *n*-propanol solution to be 50% and 87%, respectively. Stone and Reynolds [17] reported the dimeric association constant for apo AI in aqueous solution to be 1.3×10^4 M^{-1}. Therefore, at the low concentration (7×10^{-6} M) used to measured the ellipticity of apo AI, the protein is essentially monomeric. The thermal denaturation of apo AI in a pure aqueous environment exhibits a single smooth sigmoidal curve with transition mid-point (T_m) at 333°K (nevertheless a small shoulder is observable at a lower temperature, about 299°K). This thermal transition mid-point (333°K) for apo AI free in aqueous solution is similar to prior reported values [18,19].

In contrast, the thermal denaturation curve of apo AI in 30% *n*-propanol, as monitored by circular dichroism spectroscopy, is biphasic; the two transition mid-points occur at 299°K and 343°K for the first and second step of the denaturation process. The multiphasic denaturation curve indicates that there are stable intermediate structures [20] in the unfolding of apo AI solubilized in 30% *n*-propanol. As previously indicated by our cross-linking experiment at the low concentration used for our CD experiments [6], dimerisation is negligible and thus, the first step of the denaturation is not the result of the dissociation of oligomers into monomers but is the result of the denaturation of an additional folded domain induced by the presence of *n*-propanol.

Our results for the thermal denaturation of apo AI in pure aqueous solution agree also very well with the previous work of Edelstein and Scanu [21]. Interestingly, because of the lack of overlap between circular dichroism and UV spectroscopic data and of the denaturation by guanidine-HCl, these authors suspected that the denaturation process of monomeric apo AI did not obey a two states N ↔ D transition [22].

The fluorescence properties of the Trp residues, all located in the N-terminal half of apo AI (Trp^8, Trp^{50}, Trp^{72}, Trp^{108}), reported by us [6] indicated that major structural differences exist in this region of the apolipoprotein in *n*-propanol and in reconstituted HDL, on the one hand, and in water, on the other. These changes in the fluorescence properties of the Trp residues of apo AI along with the increase in α-helical content of apo AI by 37% at 4°C after addition of 30% *n*-propanol, lead us to assume that the less stable folded domain of apo AI is in fact the N-terminal half. This proposed relative instability of the N-terminal half of apo AI is consistent with the previous report of Vanloo et al. [23] which showed that the CNBr-1 fragment of human apo AI (residues 1 to 86) was less resistant to denaturation by guanidine hydrochloride. They determined the mid-points of transition for the denaturation to be approx-

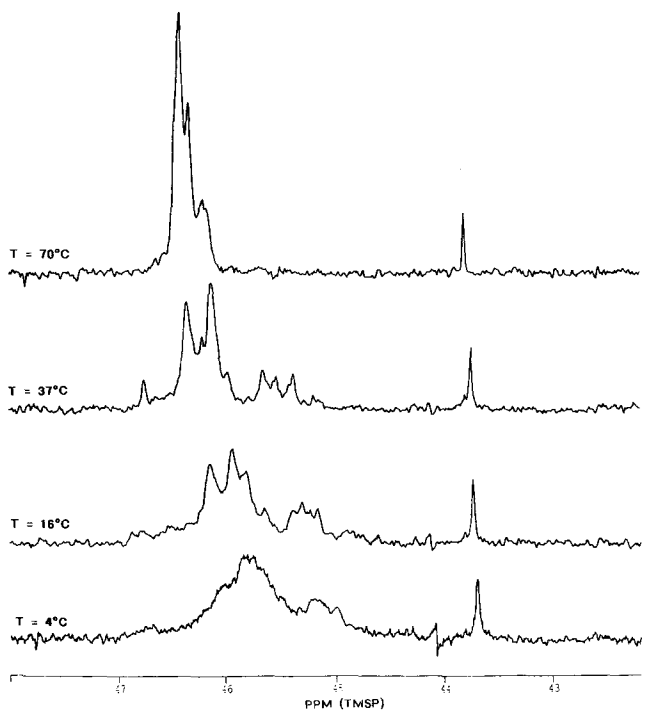

Fig. 5. Effect of temperature on the ^{13}C NMR spectra of ^{13}C dimethylated apo AI in 30% *n*-propanol, at pH 10. The temperature was maintained at 4°C, 16°C, 37°C or 70°C during the acquisition of the corresponding spectra shown from the bottom to the top of the figure, respectively.

imately 0.3 M for the CNBr-1 fragment as compared to 1 M guanidine hydrochloride for the intact apo AI solubilized in aqueous solution. They also observed a similar lower stability with the lipid associated forms, as depicted by the decrease of the mid-point of the denaturation from 4 M to 2 M for the apo AI and the CNBr-1 fragment, respectively, reassociated with phospholipids.

3.5. *Effect of the temperature on the apo AI Lys microenvironment in aqueous versus 30% n-propanol solution*

In order to investigate the structural stability of human apo AI in solution, the effect of temperature on the ^{13}C dimethyl-Lys resonance of apo AI in aqueous and in *n*-propanol solution was investigated. Fig. 5 shows the spectra of apo AI in 30% *n*-propanol at pH 10 and recorded at 4°C, 16°C, 37°C, and 70°C.

We observed complex envelopes for the ^{13}C dimethyl-Lys resonances for *n*-propanol solutions of apo AI, at 4°C, 16°C, and 37°C, that consisted of two major broad resonances from 45 ppm to 45.5 ppm and from 45.5 to 46.5 ppm, as depicted by the spectra in Fig. 5. The broad ^{13}C dimethyl-Lys resonances shift in an downfield direction when the temperature is raised. A smaller shift in a downfield direction is also observed for the dimethyl-terminal amino group resonance of apo AI with increases in temperature, as depicted by the sharp peak on the right side of the spectra in Fig. 5.

Furthermore, the ^{13}C dimethyl-Lys resonance of apo AI in propanol at 70°C becomes a sharper and less complex envelope (see the spectrum at the top of Fig. 5). This spectrum is nearly identical to the spectrum recorded at the same temperature in the presence of 8 M urea and *n*-propanol (data not shown). This is the result of the loss of the majority of the secondary structural organisation of apo AI at this temperature (see its ellipticity in *n*-propanol at 222 nm in Fig. 4). Therefore, the two major broad resonances (from 45 ppm to 45.5 ppm and from 45.5 to 46.5 ppm) collapse at 70°C into a single sharper resonance (from 46 to 46.5 ppm). This collapse of the two major broad dimethyl-Lys resonances for apo AI solubilized in *n*-propanol, was observed for temperatures that correspond to the second step of the thermal denaturation described in the preceding paragraph.

A similar downfield shift of the broad ^{13}C dimethyl-Lys resonance was observed for apo AI in aqueous solution at pH 10 when the temperature was raised. Nevertheless, the multiple peaks of the dimethyl-Lys resonance of apo AI in aqueous solution collapsed at a lower temperature (60°C) than those of apo AI in *n*-propanol solution. This result agrees with the lower thermal denaturation of apo AI in aqueous solution as depicted by the transition mid-point (T_m) of 60°C estimated from the circular dichroism data of Fig. 4.

3.6. *Implications for the future study of apo AI structure*

Several studies show that the structural properties of apo AI present on discoidal and spherical HDLs differs as well as differing from those of apo AI free in aqueous solution [6–8,18]. Sparks et al. [8] used ^{13}C NMR to probe the structure of apo AI and showed that the structure of apo AI was different when associated with discoidal or spherical HDLs and that the structure was dependent on the particle size for discs but not for spheres. The comparison of the shape of the ^{13}C dimethyl-Lys spectrum of apo AI in *n*-propanol at pH 10 (this study) to the spectrum recorded at the same pH for apo AI associated with discoidal or spherical HDLs and reported by Sparks et al. [8], shows that the native-like structure of apo AI in *n*-propanol is closer to the arrangement of apo AI on discoidal as opposed to spherical HDLs.

The present study and our previous work [6] clearly show that apo AI exhibits a higher α-helical content (~80% at 20°C) in the presence of 30% *n*-propanol than in aqueous solution (~50% at 20°C). At 4°C, pH 10, and in 30% *n*-propanol, apo AI adopts a native-like structure with characteristics (circular dichroism and ^{13}C NMR) similar to those of apo AI associated with phospholipids in large discoidal reconstituted HDLs (with 2 apo AI) as study by Sparks et al. [8,18]. These authors also observed a high α-helical content for apo AI (77%) in these particles.

At 37°C in 30% *n*-propanol we observed a decrease of the α-helicity of apo AI to 61% concomitantly with a change in the ^{13}C NMR spectrum. By ^{13}C NMR and circular dichroism spectroscopy, we observed a stable tertiary structure of apo AI in *n*-propanol at 4°C and stable intermediate structures at higher temperature.

Apo AI being essentially an interfacial protein, we call native, the lipid-bound conformation and we adopt the definition proposed by Ptitsyn [24] of a native-like molten globule as 'a compact state with native-like secondary structure and native-like tertiary fold, but without rigid tertiary structure'. The combination of our circular dichroism data, indicative of secondary structure, enzymatic digestion results [6] and ^{13}C NMR results, where the ionisation behaviour of methylated lysines probes the tertiary fold, lead us to conclude that apo AI in *n*-propanol adopts a conformation with similar secondary and tertiary fold as observed with the apo AI associated on discoidal HDLs, while keeping a certain flexibility.

Therefore, as suggested by Ptitsyn [24], it may be more relevant to speak in general of a native-like molten globule structure for apo AI in 30% *n*-propanol in order to discriminate this state from that of the disordered molten globule.

In addition to our fundamental interest in the novel behavior of interfacial proteins in solvent such as *n*-propanol, this study shows, that in 30% *n*-propanol, one native-like conformation of apo AI can be reconstituted under easily reproducible conditions. This approach will be used for subsequent experiments with apo AI mutants and for future structural studies of apo AI or apo AI fragments as well as other apolipoproteins by NMR methods. Furthermore, by changing the temperature, the hydrostatic pressure or the concentration of denaturing agents it seems also possible and easy to reconstitute other intermediate structures of apo AI that may correspond to certain lipid associated forms as reported by Sparks et al. [8]. The conformations of the lipid associated apo AI depend upon the molar ratio of phospholipids to apo AI. Our novel approach using the mixed solvent *n*-propanol/water will facilitate the study of intermediate conformations adopted by apo AI in different environmental conditions and facilitate the determination of their relative stabilities. This approach will also contribute to the characterization, the identification and the comparison of the different conformations of the lipid associated forms of apo AI.

Acknowledgements: We thank Didier Hiroux for his technical help for the purification of apo AI, Jean Dallongeville for valuable discussion

and support in this project and Lawrence Aggerberck for critical reading of the manuscript. We acknowledge the Belgian National Science foundation (NFWO) for its financial support to G. Lippens and the Fondation pour la Recherche Medicale (FRM) for its financial support to A. Leroy. We acknowledge the region Nord-Pas de Calais and Europeen Community for its financial support of the NMR laboratory at the Pasteur Institute.

References

[1] Havel, R.J. and Kane, J.P. (1989) in: The metabolic Basis of Inherited Disease (Scriver, C.R., Beaudet, A.L., Sly, W.S. and Valle, D., Eds.) 6th Edn., pp. 1129–1138, McGraw-Hill, New York.
[2] Sparrow, J.T. and Gotto, A.M. Jr. (1982) Crit. Rev. Biochem. 13, 87–107.
[3] Aggerbeck, L.P., Wettereau, J.R., Weisgraber, K.H., Mahley, R.W. and Agard, D.A. (1988) J. Mol. Biol. 202, 179–181.
[4] Wilson C., Wardell, M.R., Weisgraber, K.H., Mahley, R. W. and Agard, D.A. (1991) Science 252, 1817–1822.
[5] Weisgraber, K.H., Newhouse, Y.M. and McPherson, A. (1994) J. Mol. Biol. 236, 382–384.
[6] Leroy, A., and Jonas, A. (1994) Biochim. Biophys. Acta 1212, 285–294.
[7] Leroy, A., Toohill, K.L.H., Fruchart, J.C. and Jonas, A. (1993) J. Biol. Chem. 268, 4798–4805.
[8] Sparks, D.L., Phillips, M.C. and Lund-Katz, S. (1992) J. Biol. Chem. 267, 25830–25838.
[9] Jonas, A., Covinsky, K.E. and Sweeney, S.A. (1985) Biochemistry 24, 3508–3513.
[10] Pownall H.J. and Massey J.B.(1986) Methods Enzymol. 128, 515–518.
[11] Mezdour, H., Clavey, V., Kora, I., Koffigan, M., Barkia, A. and Fruchart, J.C. (1987) J. Chromatogr. 414, 33–45.
[12] Jentoft, N. and Dearborn, D.G. (1979) J. Biol. Chem. 254, 4359–4365.
[13] Chen, Y.H., Yang, J.T. and Martinez, H.M. (1972) Biochemistry 11, 4120–4131.
[14] Jentoft, J.E., Jentoft, N., Gerken, T.A. and Dearborn, D.G. (1979) J. Biol. Chem. 254, 4366–4370.
[15] Dick, L.R., Sherry, A.D., Newkirk, M.M. and Gray, D. M. (1988) J. Biol. Chem. 263, 18864–18872.
[16] Sherry A.D., Keepers, J. James, T.L. and Gray, D.M. (1984) Biochemistry 23, 3181–3185.
[17] Stone, W.L. and Reynolds, J.A. (1975) J. Biol. Chem. 250, 8045–8048.
[18] Sparks, D.L., Lund-Katz, S. and Phillips, M.C. (1992) J. Biol. Chem. 267, 25839–25847.
[19] Reijngoud, D.J. and Philipps, M.C. (1984) Biochemistry 23, 726–734.
[20] Ghélis, C. and Yon, J. (1982) in: Protein Folding, pp. 326–327, Academic Press, Orlando, FL.
[21] Edelstein, C. and Scanu, A. (1980) J. Biol. Chem. 255, 5747–5764.
[22] Tanford, C.(1968) Adv. Protein Chem. 23, 122–275.
[23] Vanloo, B., Morrison, J., Fidge, N, Lorent, G., Lins, L., Brasseur, R., Ruysschaert, J.M., Baert, J. and Rosseneu, M. (1991) J. Lipid Res. 32, 1253–1264.
[24] Ptitsyn, O.B. (1992) in: Protein Folding (Creighton, T.E., Ed.) pp. 243–300, Freeman, New York.